

# A First Look at Direct Measurements of $\beta^*$ in the Tevatron

M.J. Syphers

June 30, 2005

## Abstract

A direct measurement of the amplitude function across each of the Tevatron collider Interaction Regions is presented. The data were obtained during three Tevatron study periods, each dedicated to other measurements. However, the beam position data generated were found to be appropriate for the present analysis as well. This first look presumes uncoupled transverse motion, an assumption which will be lifted in future analyses. The results suggest that the values of  $\beta^*$ , the amplitude function at the Interaction Point, are near their design values of 35 cm at both detectors, in both planes and can be measured readily with the new Tevatron BPM system to an accuracy of a few percent or better.

To date, the values of the amplitude function,  $\beta$ , through the Interaction Regions of the Tevatron collider detectors during Run II have been inferred using one of two methods. First, by reconstructing event locations through the detector one can map out the luminous region and perform a least-squares fit of the beam emittance and amplitude function in each transverse degree of freedom.[1] Another method has been to perform differential closed orbit measurements while varying steering magnets in the Tevatron and producing detailed models of the synchrotron's optical properties which can reproduce the observed orbital deviations. From the modeling results one then infers the value of the amplitude function at the position monitor locations and then uses the model to ascertain values at other locations.[2] Both of these methods rely on often lengthy off-line analyses and sometimes many hours of experimental data to obtain a meaningful result.

The method employed here is to directly measure the amplitude function in the Interaction Regions using position monitors on either side of a collider experiment.[3] As the amplitude function describes the maximum extent of transverse oscillations and slopes of trajectories at a point in an accelerator, then by exciting an oscillation and measuring the position and slope, the amplitude function and its slope at that point can be extracted. This method became attractive as a new Tevatron Beam Position Monitor (BPM) system was being developed. This system is now operational,[4] and applicable turn-by-turn data are readily available during accelerator study periods. The all-new electronics allows for much higher resolution signals to be processed, including turn-by-turn data acquisition for over 8000 Tevatron revolutions at all BPM's. The improved resolution allows for meaningful measurements to be made with small amplitude beam deflections which are required during high-energy, low-beta operating conditions.

Below we describe the measurement procedure, the analysis procedure, and initial results for both experimental regions. The data are used at "face value" for this analysis, though remarks are made concerning measurement errors in a later section.

# 1 Turn-by-Turn Position Measurements

The  $\beta^*$  measurement relies on the fact that each monitor pair is separated by beam pipe with no magnetic elements in between (save the detector solenoid field, which we ignore, yet address later in a subsequent section). Thus, the simultaneous position measurement at the two BPM's provides a measurement of the slope of the trajectory at each BPM as well. By measuring turn-by-turn the position and slope of a freely oscillating particle (or, in this case, coherent motion of the beam centroid induced by a kicker magnet) one can map out a phase space trajectory and deduce the value of the amplitude function *and its slope* at that point. From this knowledge, the amplitude function across the straight section can be computed.

The position relative to the closed orbit at one BPM,  $x$ , and the slope of the trajectory relative to the closed orbit,  $x' = dx/ds$ , are related through the amplitude function *via*

$$\gamma x^2 + 2\alpha x x' + \beta x'^2 = a^2/\beta$$

where  $\alpha = -\beta'/2$ ,  $\gamma = (1 + \alpha^2)/\beta$ , and  $a$  is the amplitude of the particle motion as measured at the BPM location. The eccentricity and orientation of the phase space ellipse are given by the values of the amplitude function and its first derivative; the overall size of the ellipse is determined by the amplitude of the particle oscillation.

A transverse deflection to the beam will induce a coherent betatron oscillation which can be measured by the BPM's. However, due to inherent non-linearities in the accelerator as well as chromaticity, the phases of the oscillations of individual particles will slip and the signal will “decohere,” leading to an apparent damping of the motion. Even though the amplitude of the signal decreases, if it does so slowly enough the data will continue to lie on concentric phase space ellipses and thus can be used in the analysis. Turn-by-turn data out to about one decoherence time can provide hundreds of data points, increasing the statistics of the measurement.

Because of the tune spread which arises due to chromaticity, it is best to measure the amplitude function with “uncoalesced” beam in the Tevatron, for which the momentum spread is many times smaller. Figure 1 shows BPM measurements taken at injection of a kicked coalesced bunch and

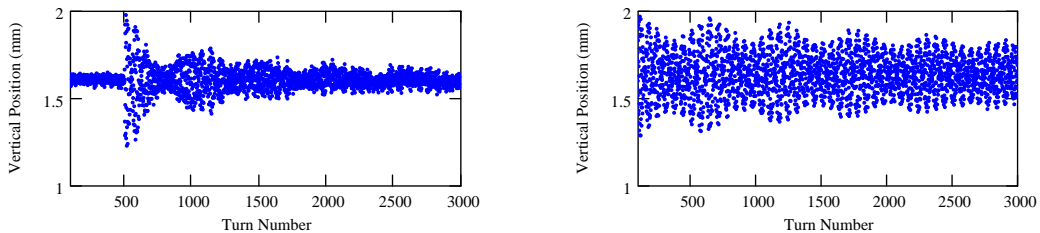


Figure 1: BPM measurements of coalesced bunches (left) and uncoalesced bunches (right).

a kicked uncoalesced bunch, for which the decoherence time is at least 10 times longer. While meaningful measurements can often be made with a few hundred turns using coalesced bunches, much greater statistical power can be gained when using uncoalesced bunches. Evident in the data are the long-term decoherence due to non-linear tune shift with amplitude and the re-coherence which occurs at the synchrotron period of about 500 turns due to residual chromaticity. (See Section 6.4.)

## 2 Data Analysis

The Tevatron BPM system now has the capability of recording 8000 turns of position data triggered on event with an rms accuracy of the data reported by the control system of about  $20 \mu\text{m}$ . As mentioned earlier, for this discussion we will ignore transverse coupling between the horizontal and vertical motion. The measurement consists of many turns of data obtained simultaneously at two BPM's on either side of the interaction region long straight section, as depicted in Figure 2. At

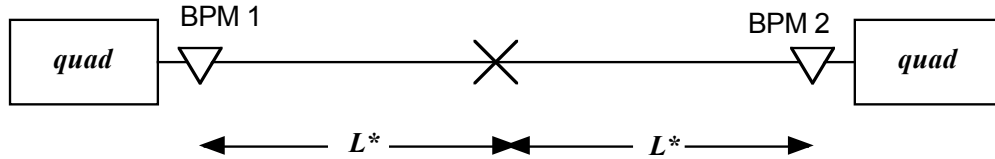


Figure 2: Schematic of long straight section across Interaction Point.

each IR the vertical detectors are separated by  $\pm 14.8 \text{ m}$  and the horizontal detectors by  $\pm 15.0 \text{ m}$  from the center of the straight section. By taking simple sums of the data from a pair of BPM's the amplitude function and its slope can be determined at each BPM, and the values in between computed.

### 2.1 Moments and End Points

In one degree of freedom, the transverse motion at a BPM on turn number  $n$  is given by

$$x_n = A\sqrt{\beta}\sin(\delta + 2\pi\nu n)$$

where  $A$  and  $\delta$  are determined by the initial conditions of the oscillation due to the applied kick, and  $\nu$  is the betatron tune. The slope of the oscillation at the BPM is given by

$$x'_n = -\frac{A}{\sqrt{\beta}}[\alpha \cos(\delta + 2\pi\nu n) + \sin(\delta + 2\pi\nu n)].$$

Averaging over phases or, equivalently, averaging data over a large number of turns, we find that

$$\langle x^2 \rangle = \frac{1}{2} A^2 \beta, \quad \langle x'^2 \rangle = \frac{1}{2} A^2 \gamma.$$

Taking the correlation of  $x$  and  $x'$  we get

$$\langle xx' \rangle = -\frac{1}{2} A^2 \alpha$$

and so the data can be used to extract the value of  $\beta$  and its slope  $\beta' = -2\alpha$  at the BPM. As for the constant  $A$  above, one can easily verify that

$$\frac{1}{2} A^2 = \sqrt{\langle x^2 \rangle \langle x'^2 \rangle - \langle xx' \rangle^2}.$$

The angle  $x'$  is determined by knowing the distance  $2L^*$  between two BPM's and measuring the positions at the two BPM's  $x_1$  and  $x_2$  simultaneously. Since there are no intervening magnetic gradients, then

$$x' = \frac{x_2 - x_1}{2L^*}.$$

The final results for  $\beta$  and  $\alpha$  at the BPM at each end of the straight section is then,

$$\begin{aligned} \beta_1 &= \frac{2\langle x_1^2 \rangle L^*}{\sqrt{\langle x_1^2 \rangle \langle x_2^2 \rangle - \langle x_1 x_2 \rangle^2}}, & \beta_2 &= \frac{2\langle x_2^2 \rangle L^*}{\sqrt{\langle x_1^2 \rangle \langle x_2^2 \rangle - \langle x_1 x_2 \rangle^2}}, \\ \alpha_1 &= \frac{\langle x_1^2 \rangle - \langle x_1 x_2 \rangle}{\sqrt{\langle x_1^2 \rangle \langle x_2^2 \rangle - \langle x_1 x_2 \rangle^2}}, & \alpha_2 &= -\frac{\langle x_2^2 \rangle - \langle x_1 x_2 \rangle}{\sqrt{\langle x_1^2 \rangle \langle x_2^2 \rangle - \langle x_1 x_2 \rangle^2}}. \end{aligned}$$

## 2.2 The Amplitude Function Across the IR

Since we have a drift space between the two BPM's we know that the function  $\gamma = (1 + \alpha^2)/\beta$  is a constant and the amplitude function is parabolic and of the form

$$\begin{aligned} \beta(s) &= \beta_1 - 2\alpha_1 s + \gamma s^2 &= \beta_2 - 2\alpha_2(s - 2L^*) + \gamma(s - 2L^*)^2; & \text{ additionally,} \\ \alpha(s) &= \alpha_1 - \gamma s &= \alpha_2 - \gamma(s - 2L^*), \end{aligned}$$

where  $s$  is the distance from the upstream BPM. The minimum of the amplitude function and its location relative to the upstream BPM are

$$\check{\beta} = \frac{2L^*}{\alpha_1 - \alpha_2} \quad \text{at} \quad \check{s} = \frac{2\alpha_1 L^*}{\alpha_1 - \alpha_2}.$$

Henceforth, we will refer to the minimum value of  $\beta$  as  $\beta^*$ , which may or may not be centered in the straight section. The distance to the minimum from the center of the straight section is

$$\Delta s^* = \check{s} - L^* = \frac{\alpha_1 + \alpha_2}{\alpha_1 - \alpha_2} L^*.$$

### 3 Measurements at 150 GeV, 2005 May 2

During a studies period of 2005 May 2, turn-by-turn data were obtained at the injection energy of 150 GeV, under the “injection optics” configuration for which the design value of  $\beta^*$  is 150 cm in each plane, at each IP.[5] Two sets of data were taken, one with a horizontal kick applied to the beam, another with a vertical kick. Thirty uncoalesced bunches were used in each case, with typical bunch intensities of  $\sim 10^{10}$  per bunch. Chromaticities were set to  $\xi_h \approx 3.5$ ,  $\xi_v \approx 2.5$ , and the minimum tune separation was  $\Delta\nu_{min} \approx 0.003$ . Figure 3 shows the first 2000 turns of the horizontal BPM data from the CDF straight section and the D0 straight section for a horizontal kick, with the mean subtracted. Similarly, Figure 4 is for the vertical BPM data during a vertical kick. (The tune in this case was very near  $4/7$ .) Figure 5 shows the reconstruction of the phase space for the upstream CDF horizontal detector using the first 6000 turns as an example. The ellipse in the figure corresponds to the values of  $\beta$  and  $\alpha$  obtained directly from the analysis described above. Figure 6 shows the same data, but only turns 0-100 (outer points) and turns 6000-6100 (inner points). As can be seen, the orientation of the apparent phase space ellipse does not change over time.

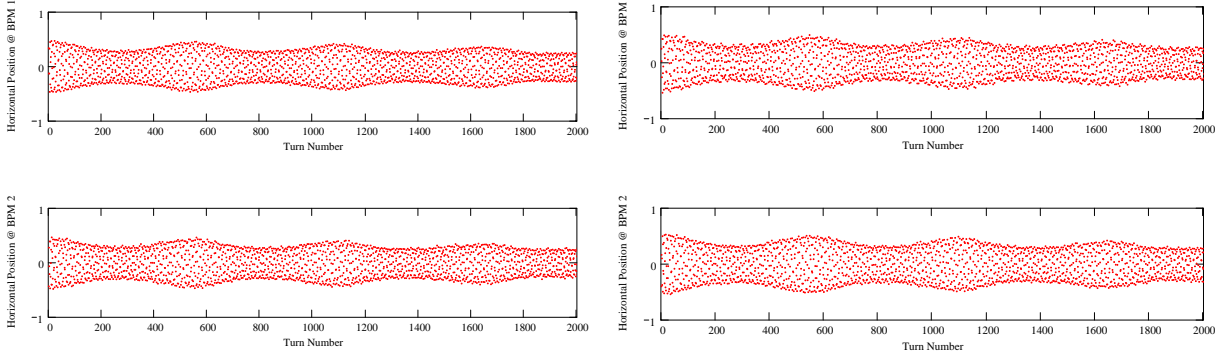


Figure 3: Horizontal BPM data,  $x_1$  (top) and  $x_2$  (bottom), at CDF (left) and D0 (right) for a horizontal applied kick at injection energy of 150 GeV. The horizontal tune was 20.586. For CDF,  $\langle x_1 \rangle = 1.6$  mm,  $\langle x_2 \rangle = 6.6$  mm; for D0,  $\langle x_1 \rangle = 3.0$  mm,  $\langle x_2 \rangle = -0.3$  mm.

Performing the straightforward analysis described in Section 2 yields the amplitude functions depicted in Figure 7. The values at the BPM’s, the values of the minima, and the locations of the minima are provided in Table 1.

Table 1: Amplitude Functions at Injection

		$\beta_1$	$\beta_2$	$\beta^*$	$\Delta s^*$
<b>CDF</b>	Hor	41.2 m	40.1 m	144 cm	+5.49 cm
	Ver	31.0 m	33.2 m	181 cm	-13.4 cm
<b>D0</b>	Hor	40.2 m	46.0 m	136 cm	-26.1 cm
	Ver	31.2 m	30.6 m	189 cm	+3.56 cm

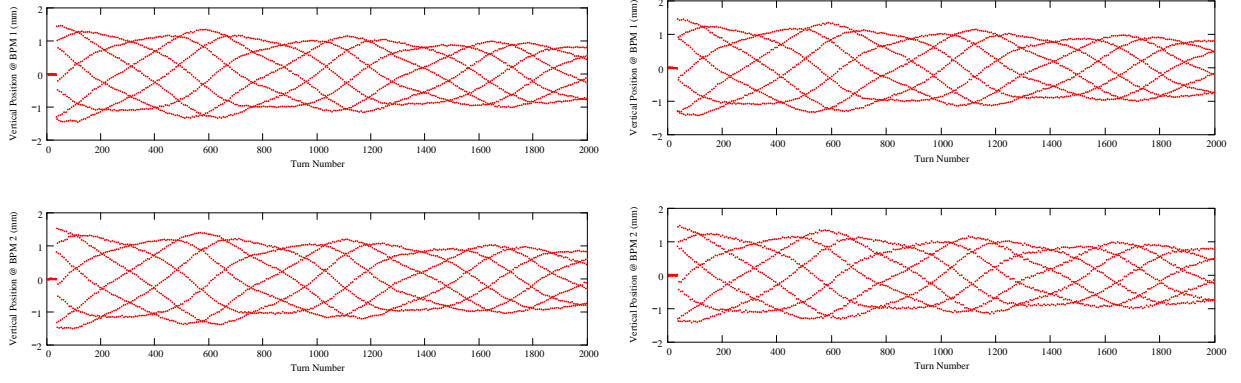


Figure 4: Vertical BPM data,  $y_1$  (top) and  $y_2$  (bottom), at CDF (left) and D0 (right) for a vertical applied kick at injection energy of 150 GeV. The vertical tune was 20.571. For CDF,  $\langle y_1 \rangle = -0.8$  mm,  $\langle y_2 \rangle = 1.4$  mm; for D0,  $\langle y_1 \rangle = -1.4$  mm,  $\langle y_2 \rangle = 2.0$  mm.

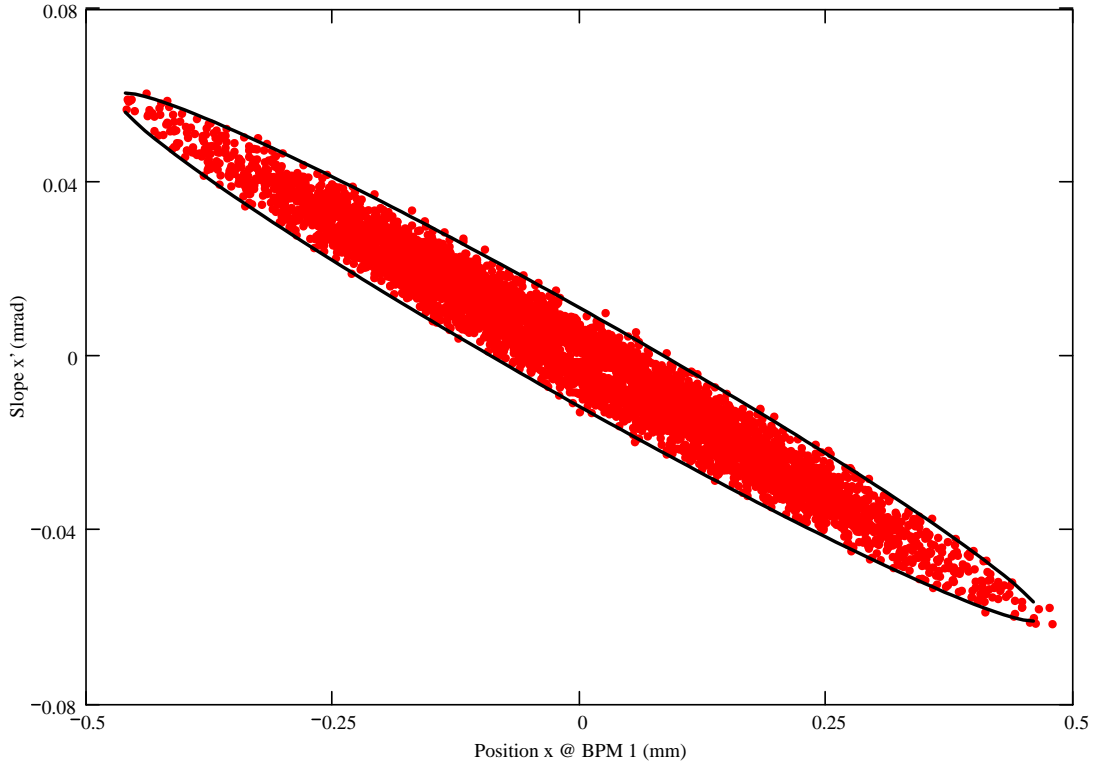


Figure 5: Horizontal phase space at the upstream CDF detector taken using  $x_1$  and  $x_2$  data in the left-hand portion of Figure 3. The ellipse corresponds to  $\beta_1 = 41.2$  m and  $\alpha_1 = 5.26$ , a result using the first half of the data (3000 turns) in the analysis.

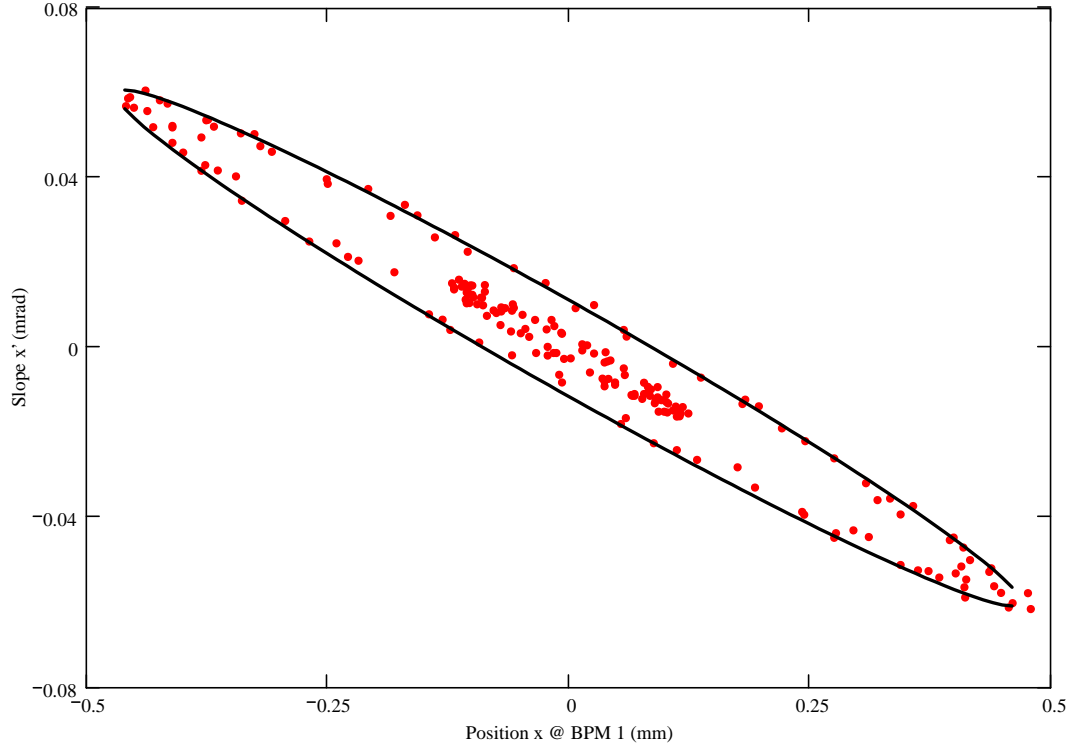


Figure 6: Same as Figure 5, but only showing data for turns 0-100 and turns 6000-6100 of the original data set. The ellipse is the same curve as in Figure 5.

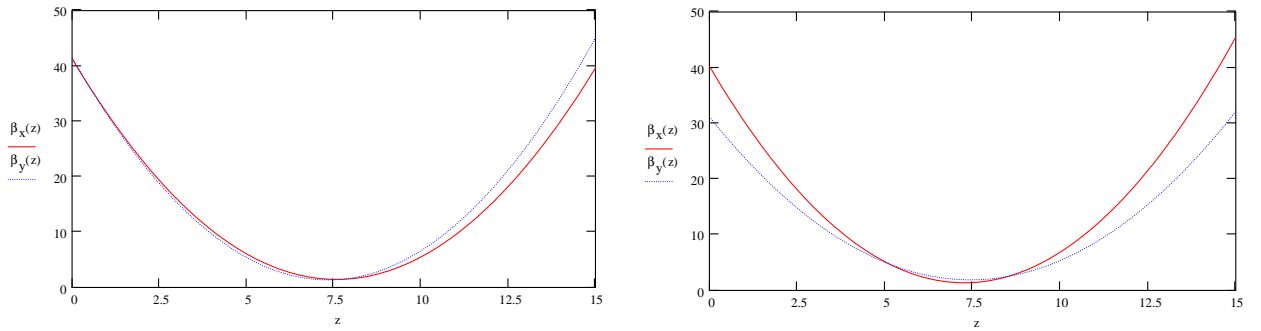


Figure 7: Amplitude functions at (left) CDF and (right) D0 at injection.

## 4 Measurements at 980 GeV, 2005 May 31

Another set of data was taken during a study period on 2005 May 31 during 980 GeV operation.[6] In this case, the deflections occurred with “low-beta” optics, or “collision optics,” used during a store. The design value for  $\beta^*$  in this configuration is 35 cm.

During this study coalesced bunches were used, as they would be during a store. Thus, the momentum spread was large and the decoherence was much stronger due to chromaticity as well as due to the stronger non-linear fields experienced with the low-beta optics. While 8000 turns of data were taken, only 250 are used in the analysis of the horizontal motion and only 125 are used for the vertical. The data are shown in Figures 8 and 9. The corresponding values for the amplitude functions derived from the data are given in Table 2. Errors assigned are discussed in Section 6.

Table 2: Analysis at 980 GeV, using 250 turns for the horizontal, and 125 turns for the vertical.

		$\beta_1$	$\beta_2$	$\beta^*$	$\delta\beta^*$	$\Delta s^*$	$\delta\Delta s^*$
<b>CDF</b>	Hor	173 m	141 m	35 cm	$\pm 1$ cm	+40 cm <sup>†</sup>	$\pm 1$ cm
	Ver	164 m	165 m	33 cm	$\pm 1$ cm	-2.4 cm	$\pm 1$ cm
<b>D0</b>	Hor	151 m	149 m	35 cm	$\pm 3$ cm	+1.6 cm	$\pm 1$ cm
	Ver	153 m	150 m	36 cm	$\pm 1$ cm	+3.5 cm	$\pm 1$ cm

<sup>†</sup>see Section 6.1

## 5 Measurements at 980 GeV, 2005 June 23

A third data set was obtained on 2005 June 23 at 980 GeV, this time using uncoalesced bunches.[7] Figure 10 shows representative horizontal and vertical data for this pass. While the chromatic decoherence was pronounced, it was still viable to use  $\sim 1,500$  turns in the analysis, 5-10 times the number of turns used for the data obtained using coalesced bunches. The results are displayed in Table 3. We see that on this day the values of  $\beta_y$  are again measured with good precision, giving 1-2% values at each IP. However, the results for  $\beta_x$  vary with the number of turns used. More will be said about this in the next section.

Table 3: Amplitude Functions at 980 GeV, 2005 June 23, using 1500 turns.

		$\beta^*$	$\delta\beta^*$	$\Delta s^*$	$\delta\Delta s^*$
<b>CDF</b>	Hor	34.6 cm	$\pm 0.6$ cm	+34.2 cm <sup>†</sup>	$\pm 0.4$ cm
	Ver	38.7 cm	$\pm 0.3$ cm	-4.8 cm	$\pm 0.4$ cm
<b>D0</b>	Hor	38.7 cm	$\pm 1.6$ cm	+1.1 cm	$\pm 0.4$ cm
	Ver	40.3 cm	$\pm 0.2$ cm	+2.3 cm	$\pm 0.2$ cm

<sup>†</sup>see Section 6.1



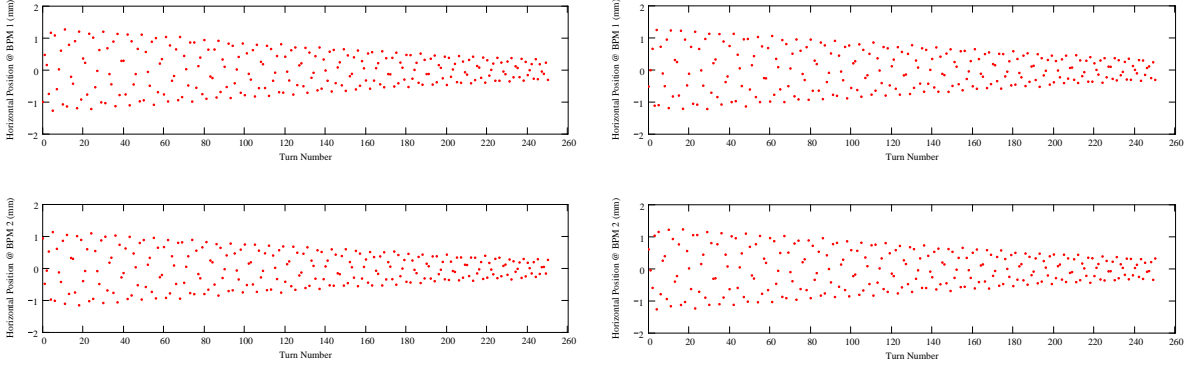


Figure 8: Horizontal BPM data at CDF (left) and D0 (right) for a kick at 980 GeV. Here,  $\nu_x = 20.580$ . At CDF,  $\langle x_1 \rangle = 0.10$  mm,  $\langle x_2 \rangle = 7.8$  mm; at D0,  $\langle x_1 \rangle = -0.15$  mm,  $\langle x_2 \rangle = 2.5$  mm.

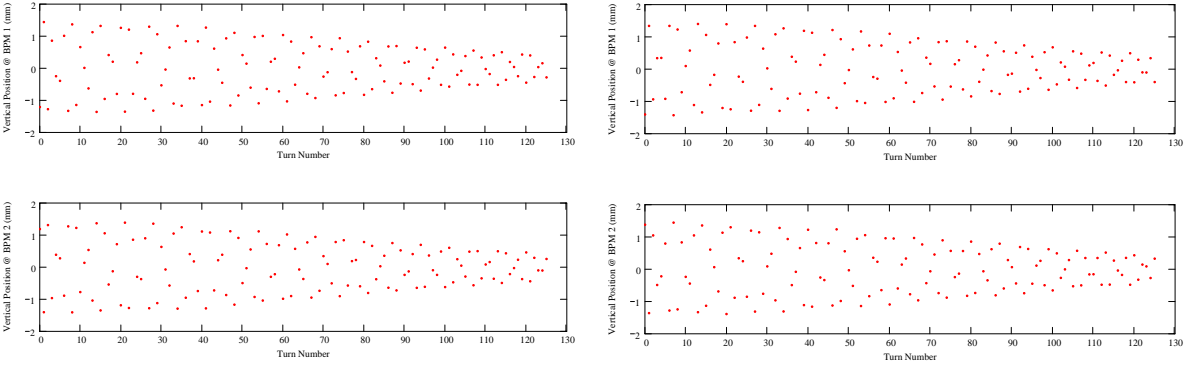


Figure 9: Vertical BPM data at CDF (left) and D0 (right) for a vertical kick at 980 GeV. Here,  $\nu_y = 20.577$ . For CDF,  $\langle y_1 \rangle = -1.0$  mm,  $\langle y_2 \rangle = 1.6$  mm; for D0,  $\langle y_1 \rangle = -2.0$  mm,  $\langle y_2 \rangle = 0.62$  mm.

## 6 Notes on Measurement Errors

The rms readback error of the BPM system is on the order of  $20 \mu\text{m}$ . The oscillations induced for the measurements above were typically on the order of 1 mm. Thus, one would expect an error on  $\beta^*$  of approximately 2% with this resolution. The final value of  $\beta^*$  also depends upon our knowledge of  $L^*$ . The distances between the BPM centers are known to better than a centimeter, or  $< 0.1\%$

One of the next questions to be asked of the technique above is its dependency on the number of turns used in the analysis. For the injection data, with several thousand turns of useable numbers, this isn't so much an issue. But when only a few hundred turns are used, this must be questioned. Figure 11 plots the computed value of  $\beta^*$  at 980 GeV *vs.* the number of turns,  $N_{turns}$  used in the analysis. The vertical lines in the plots indicate the decoherence time (where the coherent amplitude is reduced by a factor of about  $1/e$ ). The computations of  $\beta_y^*$  vary by only about  $\pm 2\%$  up through 250 turns. Horizontally, the value of  $\beta_x^*$  seems to have the same constancy for CDF ( $\sim \pm 3\%$ ) out to the decoherence time, though a general trend to diverge with  $N_{turns}$  is seen. For

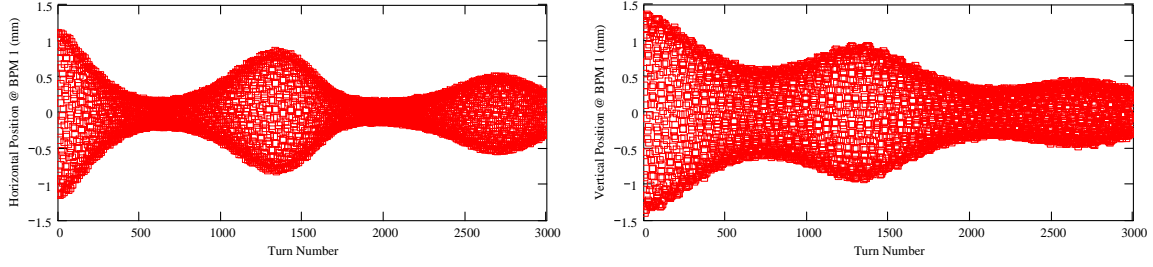


Figure 10: Data taken on 2005 June 23. Left:  $x_1$  at CDF. Right:  $y_1$  at D0.

the D0 calculation the divergence is more pronounced. Still, however, the D0 result varies by only  $\pm 7\%$  for up to 125 turns used. For comparison, Figure 12 shows the same analysis for the injection data sets; clearly more turns, with correspondingly longer decoherence time, is preferred.

Similar plots are made for the June 23 data set in Figure 13. Here, we again see a constancy in the vertical results, over several thousand turns, just as in the injection data. However, the horizontal results again appear to diverge. Upon closer inspection of the horizontal data, we see two effects. First, there is a large chromaticity which means that the measurement is less reliable when using data points during the decoherence stages. Also, it is apparent that there is a low frequency movement of the closed orbit at the BPM's on the scale of  $100\text{-}200\text{ }\mu\text{m}$ . (Motion of the vertical closed orbit is 2-4 times smaller.) This is reflected in Figure 14, which plots a running 100-turn average over the data. The closed orbit motion obviously alters the results, and will be investigated in a future analysis.

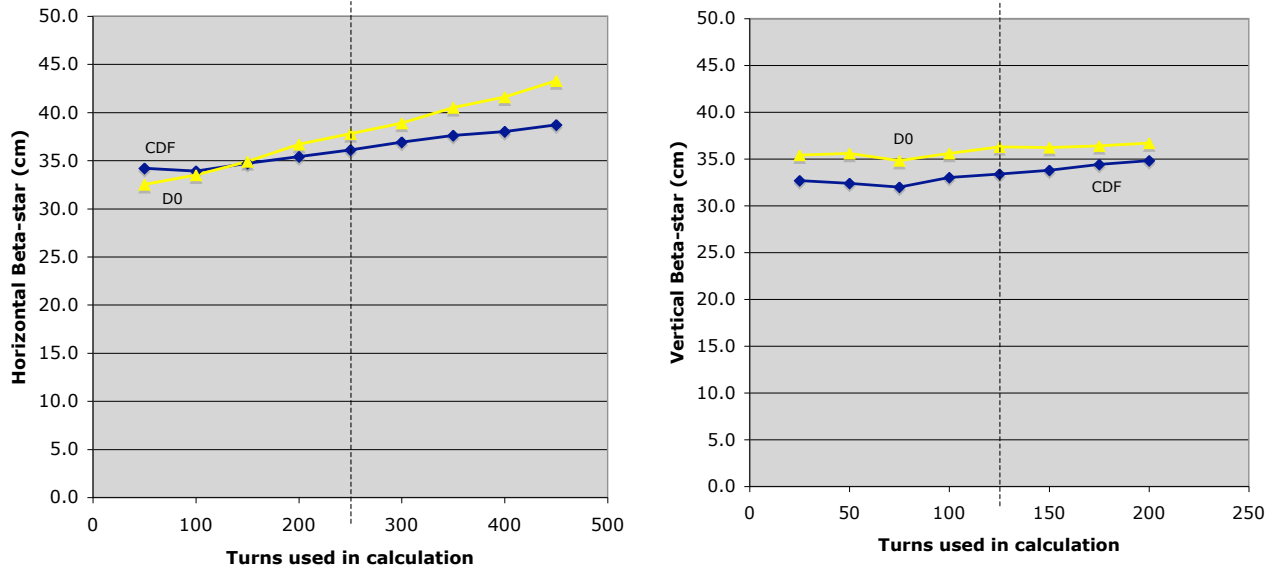


Figure 11: Computed  $\beta^*$  vs.  $N_{turns}$  for 980 GeV data taken June 31.

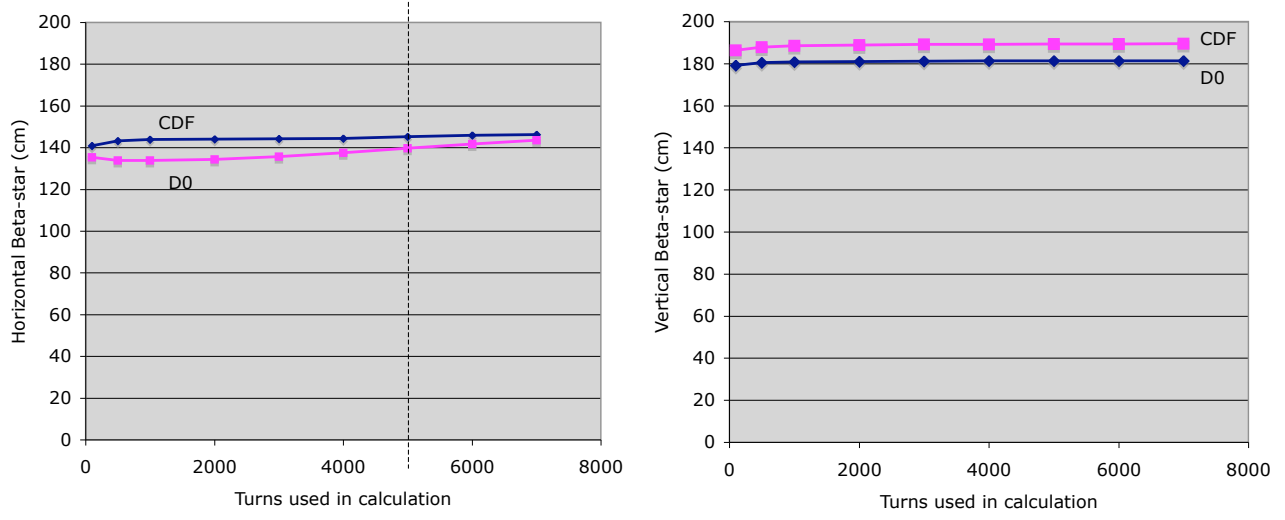


Figure 12: Computed  $\beta^*$  *vs.*  $N_{turns}$  for 150 GeV data.

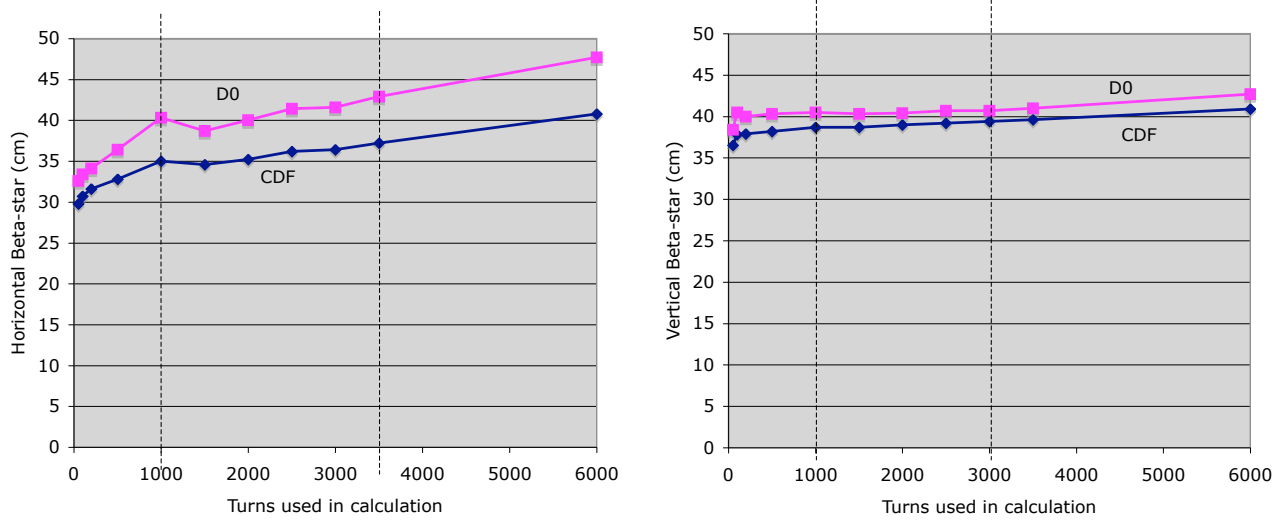


Figure 13: Computed  $\beta^*$  *vs.*  $N_{turns}$  for 980 GeV data with uncoalesced beam.

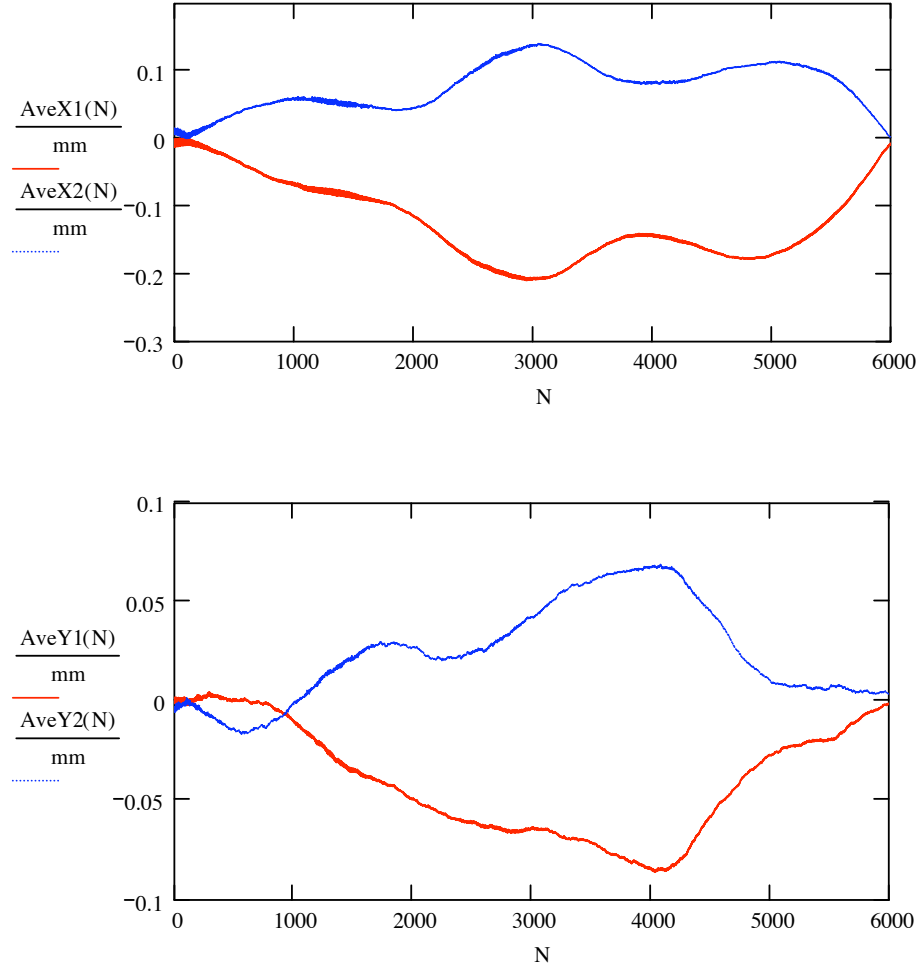


Figure 14: A 100-turn running average performed on the D0 downstream BPM data for the June 980 GeV measurement, indicating closed orbit drift.

## 6.1 Effect of BPM Scaling

The computations indicate that the low-beta optics is tuned close to design, with  $\beta^*$  near 35 cm and the waists situated within a few centimeters of the middle of the straight section. The exception appears to be  $\beta_x^*$  at the CDF detector. Here, the data suggest the waist is off by 40 cm. Upon closer inspection it has been noticed that the downstream horizontal BPM at B0 was reading back a closed orbit position of approximately 8 mm (with maximum excursions, therefore, of about 9 mm). All 7 other detectors had the beam centered to about 2 mm or better. It is known that the response of the BPM is non-linear with position. The present scaling of the readback position from the new BPM system is given by

$$x = 26.18 \frac{A - B}{A + B} \quad [\text{mm}]$$

where  $A$  and  $B$  are the induced voltages on the two plates of the pickup. (A survey offset has been ignored.) The sensitivity of the device will be reduced by several percent and the reading will be too low at this size beam offset by as much as 10-20%.[8] Recent beam measurements by M. Martens[9] also validate effects of this magnitude.

To understand the effect of scaling we perform a short sensitivity analysis as follows. Consider a measurement with perfect BPM's, where the beam waist is centered. In this case,  $\langle x_1^2 \rangle = \langle x_2^2 \rangle \equiv \sigma$ , and let  $\langle x_1 x_2 \rangle \equiv c$ . Then,  $\alpha_1 = -\alpha_2 = \sqrt{(\sigma - c)(\sigma + c)}$ . Thus, our analysis would report back

$$\beta^* = L^* \sqrt{\frac{\sigma + c}{\sigma - c}}, \quad \Delta s^* = 0.$$

We next suppose that the downstream BPM is off by a scale factor  $r = 1 - \delta$ ; then we would obtain

$$\begin{aligned} \tilde{\alpha}_1 &= \frac{\sigma - rc}{r\sqrt{\sigma^2 - c^2}} & \tilde{\alpha}_2 &= -\frac{r^2\sigma - rc}{r\sqrt{\sigma^2 - c^2}} \\ \tilde{\alpha}_1 - \tilde{\alpha}_2 &= \frac{(1 + r^2)\sigma - 2rc}{r\sqrt{\sigma^2 - c^2}} & \tilde{\alpha}_1 + \tilde{\alpha}_2 &= \frac{(1 - r^2)\sigma}{r\sqrt{\sigma^2 - c^2}} \end{aligned}$$

from which the change in the waist position and the relative change in  $\beta^*$  are found to be

$$\begin{aligned} d\Delta s^* &= \frac{1 - r^2}{1 + r^2 - 2r(c/\sigma)} L^* \\ \frac{d\beta^*}{\beta^*} &= -\frac{(1 - r)^2}{1 + r^2 - 2r(c/\sigma)}. \end{aligned}$$

In terms of  $\delta = 1 - r \ll 1$ ,

$$d\Delta s^* \approx \frac{L^*}{2} \cdot \delta, \quad \frac{d\beta^*}{\beta^*} \approx -\frac{1}{4}\delta^2.$$

So, if the downstream BPM at CDF is reading back 10% too low, for example, then the BPM readback would lead to a misinterpretation of the waist position on the order of  $(7.5 \text{ m}/2) \cdot (0.1) = 38 \text{ cm}$ , while the numerical value of  $\beta^*$  would only be affected by  $-0.25\%$ . The fact that the only outcome with a large displacement of the waist is also the only location with a large offset at a detector is compelling. And, in addition, the sign is right.

## 6.2 Influence of the Detector Solenoid Field

While the positions are directly measured, the determination of the slope of the beam trajectory across the straight section has assumed no external fields exist between the two monitors. In reality, each detector has a solenoid field through this region. The CDF solenoid has a length of  $\ell = 4.8$  m with a central field strength  $B_s = 1.5$  T. For the D0 solenoid,  $\ell = 2.7$  m and  $B_s = 2.0$  T. The characteristic angle,  $\theta = B_s \ell / B\rho$ , takes on the value  $\theta = 11$ -14 mrad at 150 GeV and  $\theta = 1.7$ -2.2 mrad at 980 GeV for D0 and CDF respectively. The effect of a solenoid on the trajectory of a particle, for small  $\theta$ , is given by

$$\begin{pmatrix} x_2 \\ x'_2 \\ y_2 \\ y'_2 \end{pmatrix} = \begin{pmatrix} 1 & \ell & \frac{1}{2}\theta & -\frac{1}{2}\theta\ell \\ 0 & 1 & 0 & \frac{1}{2}\theta \\ -\frac{1}{2}\theta & \frac{1}{2}\theta\ell & 1 & \ell \\ 0 & -\frac{1}{2}\theta & 0 & 1 \end{pmatrix} \begin{pmatrix} x_1 \\ x'_1 \\ y_1 \\ y'_1 \end{pmatrix}$$

from which we see that, compared to traversal of a pure drift space of length  $\ell$ , the resulting change in slopes due to the solenoid are

$$\begin{aligned} \Delta x' &= \frac{1}{2}\theta y'_1, \\ \Delta y' &= -\frac{1}{2}\theta x'_1. \end{aligned}$$

Using the larger value  $\theta = 0.0022$  above for 980 GeV, we see that for a horizontal kick where the amplitude of the vertical motion is at most  $\sim 20\%$  of the horizontal amplitude (as seen in the data taken at 980 GeV), then

$$\frac{\Delta x'}{\hat{x}'} = \frac{1}{2}\theta \left( \frac{\hat{y}'}{\hat{x}'} \right) = \frac{1}{2}(0.0022) \left( \frac{1}{5} \right) = 0.02\%.$$

At injection, where the coupling is observed to be only  $\sim 10\%$ ,  $\Delta x' / \hat{x}' \approx 0.07\%$ . Thus, while the solenoid may affect the coupled motion of the particles (the two detectors generate a minimum tune split at injection of  $\Delta\nu_{min} \approx 0.003$ , for example), the effect of the solenoid field on the measurement of a single trajectory across an IR is completely negligible. Should a measurement be made, as will be proposed later, with kicks in both degrees of freedom simultaneously, then the relative error on the  $x'$  measurement still would be only  $\sim 0.1\%$ .

## 6.3 Effect of Beam-Beam Interaction on the Amplitude Function

It needs to be pointed out that one major difference between the measurements discussed here (as well as differential orbit measurements) and the deduction of  $\beta^*$  from the detector luminous region reconstruction is that in the latter the beams are actually colliding. In this case, the beam-beam interaction takes place at each IP, and acts as a focusing lens on each beam. To lowest order, the focal length of the “lens” is given by

$$\frac{1}{f} = 4\pi\xi/\beta^*$$

where  $\xi$  is the “beam-beam parameter,”  $\xi \equiv 3Nr_0/2\epsilon_N$ , where  $N$  is the number of particles per bunch,  $\epsilon_N$  is the 95% normalized emittance, and  $r_0$  is the classical radius of the proton. For  $\xi \sim 0.01$ , then  $f \sim 3$  m.

A gradient error of focal length  $f$  introduced where  $\beta = \beta_0$  produces a perturbation of the amplitude function around the accelerator of amplitude

$$\left| \frac{\Delta\beta}{\beta} \right| \approx \frac{\beta_0/f}{2|\sin 2\pi\nu|} = \frac{2\pi\xi}{|\sin 2\pi\nu|}$$

and at the location of the error has magnitude  $-(\beta_0/f) \cot(2\pi\nu)/2 = -2\pi\xi \cot(2\pi\nu)$ . So, for  $\xi = 0.01$ ,  $\Delta\beta^*/\beta^* = -12\%$ , and the wave around the ring is of amplitude 13% (using  $\nu = 20.578$ ).

Additionally, all else being perfect (which, of course, is not the case), the two IP’s should be separated by a betatron phase advance of  $2\pi$ , meaning that the two beta-waves generated at the IP’s will tend to cancel in between the two IP’s and add outside. Thus, the amplitude function distortion due to the beam-beam interaction would generate a degree of asymmetry across the luminous region. Naturally, other gradient errors in the accelerator may act to mask this effect, including the 70 other long-range beam-beam interactions along the way. The point is that the measurement conditions are quite different with and without the on-coming beam in the accelerator, and so  $\sim 10\%$  differences between results of the two methods of measuring  $\beta^*$  should not be too surprising.

## 6.4 Nonlinear De-tuning and Chromaticity

The decoherence of the BPM signal of a kicked beam can be characterized analytically for a Gaussian beam. The result for turn number  $n$  is[10]

$$\bar{x}(n) = a \cdot e^{-[2\sigma_s\xi\nu_s^{-1}\sin(\pi\nu_s n)]^2/2} \cdot \left( \frac{1}{1 + (\nu_p n)^2} e^{-\frac{a^2}{2\sigma^2} \frac{(\nu_p n)^2}{1 + (\nu_p n)^2}} \right) \cdot \cos[2\pi\nu_0 n + \Delta\bar{\phi}(n)] \quad (1)$$

where  $a$  is the amplitude of the induced betatron oscillation,  $\nu_0$  the betatron tune,  $\nu_s$  the synchrotron tune,  $\sigma$  the transverse rms beam size,  $\sigma_s$  the rms relative momentum spread,  $\xi$  the chromaticity, and  $\nu_p$  the non-linear detuning parameter. (If the tune varies with amplitude according to  $\nu = \nu_0 - Ka^2$ , then  $\nu_p = 4\pi K\sigma^2$ .) The centroid phase shift is  $\Delta\bar{\phi}$ , which develops over time as well.

When examining the turn-by-turn data one can ascertain several of the above parameters. For example, in the data presented here, the beam was typically kicked several units of  $\sigma$ , and the amplitude  $a$  is essentially the maximum deviation over the first few turns. The beam decohered and recohered at roughly the synchrotron tune due to chromaticity, so this parameter can be inferred as well. By adjusting the product  $\xi \cdot \sigma_s$  one can match the depth of the decoherence due to the synchrotron motion. Finally, the overall envelope is adjusted using  $\nu_p$ .

Figure 15 shows the first 3000 turns of data for the downstream vertical BPM at D0 during the June 980 GeV study. The curves represent the “envelope” from Equation 1, using  $\nu_p = 0.00018$ ,  $a = 1.34$  mm,  $\xi\sigma_p = 0.00043$ , and  $\nu_s = 1/1370$ , all fit by hand as described in the preceding

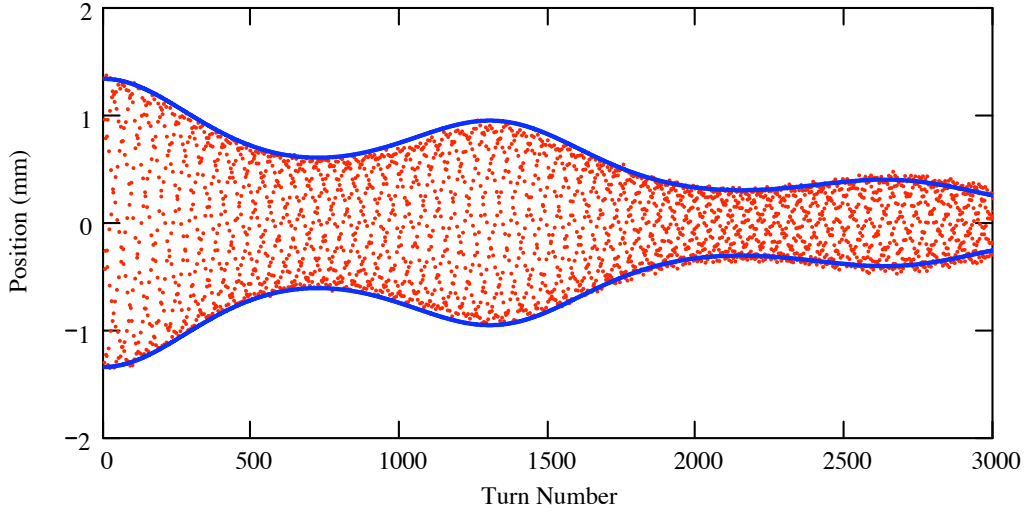


Figure 15: Decoherence of BPM signal, and computed “envelope” discussed in the text.

paragraph. The new BPM system opens up the possibilities of performing precision measurements of non-linear beam behavior and chromatic effects with much greater precision than ever before at the Tevatron.

## 7 Conclusions

Using the newly upgraded Tevatron BPM system, direct measurements of the amplitude function across the two interaction region straight sections have been performed. The technique involves inducing coherent betatron oscillations and recording turn-by-turn position measurements at two BPM’s in each plane. A fast and simple analysis provides determination of  $\beta^*$  to a few percent accuracy, and the results indicate the values, at least in one measurement, were very close to design. The data used in this analysis were obtained for other purposes, but were quite adequate for this first investigation of the method.

It was found that the non-linear response of the BPM signal with position needs to be incorporated into the control system database to deal with measurements involving offsets of 8 mm or so, as is currently present at the CDF detector. Also evident was a slow, several-hundred-micron movement of the closed orbit during the measurement, which may also be affecting the computed values of  $\beta_x$ . Hopefully this can easily be addressed with an appropriate pre-processing of the data to improve the measurement.

At the time of this writing, only one set of measurements at injection and two at low-beta have been analyzed. Dedicated studies need to be performed to understand the reproducibility of the method and to nail down further error sources. The Tevatron conditions should be well tuned



and documented, such as closed orbits, tunes, coupling, chromaticity, emittances, and intensities, before the measurements are performed. (In fact, initial measurements would actually be used as diagnostics to do the tune-up!) Then, a series of data sets for horizontal kicks, vertical kicks, and combinations of both should be performed for a range of kick amplitudes. One should be able to find an optimal procedure for measuring  $\beta^*$ , pitting longer decoherence times and more statistics with short amplitude kicks *vs.* better relative accuracy for the position data with larger amplitude kicks.

Additionally, the effects of coupling will need to be incorporated into the analysis. By kicking the beam vertically and horizontally simultaneously and recording data, the full  $4 \times 4$  matrix parameters at a BPM location can be inferred and the full development of the beam envelope through the straight section in the presence of global coupling can be computed. Ultimately, to aid in the above, a console application code needs to be written.

The improved BPM system opens the door to other possible studies as well. For example, one could study the variation of  $\beta^*$  with closed orbit deviations throughout the Tevatron, or  $\beta^*$  variation with momentum. The application code, once written, can be used to tune up the waist location, using the  $\alpha$ -bump knobs, during shot set-ups. It may be possible to investigate beam-beam effects, such as  $\beta^*$  with and without beam-beam, by performing special studies with one proton bunch and one anti-proton bunch in the ring. Many other possibilities undoubtedly exist.

The author would like to thank Yuri Alexahin, Eleina Gianfelice-Wendt, and Vahid Ranjbar for pointing him to the various data sets used here, Vic Scarpine for his help in obtaining pre-BPM upgrade data for initial testing of the idea, and Mike Martens, Leo Michelotti, and Rob Kutschke for many useful discussions. Also, thanks to Vaia Papadimitriou for asking the question in the first place.

## References

- [1] J. Slaughter, J. Estrada, K. Genser, A. Jansson, P. Lebrun, J.C. Yun, S. Lai, “Tevatron Run II Luminosity, Emittance and Collision Point Size,” Proc. 2003 Part. Accel. Conf., 0-7803-7739-7, 1763-1765 (2003); also, “Luminosity Task Force” home page, [http://www-bd.fnal.gov/SDA\\_Viewer/VaiaLuminosity/index.html](http://www-bd.fnal.gov/SDA_Viewer/VaiaLuminosity/index.html) .
- [2] V. Lebedev, “Measurement and Correction of Low-Beta Optics At Tevatron,” presentation at Fermilab, 2004 July 29, Fermilab internal document, Beams-doc-1313.
- [3] M.J. Syphers, “Determining Beta-Star in the Tevatron,” Fermilab Report, Beams-doc-1088 (March 2004).
- [4] S. Wolbers, *et al.*, “Tevatron Beam Position Monitor Upgrade,” presented at 2005 Particle Accelerator Conference, Knoxville (May 2005); M. Martens, *et al.*, “Tevatron Beam Position Monitor Upgrade Requirements,” Fermilab Report, Beams-doc-554 (2003).
- [5] M. Martens, V. Ranjbar, E. Gianfelice-Wendt, Tev Studies, eLog entry, 2005 May 2.
- [6] V. Ranjbar, C.Y. Tan, Tev Studies, eLog entry, 2005 May 31.

- [7] Y. Alexahin, Tev Studies, eLog entry 2005 June 23.
- [8] R. Shafer, “Sensitivity of Beam Position Detectors for the Tevatron,” Fermilab Report, UPC-101 (May 1979); R. Shafer, R. Webber, T. Nicol, “Fermilab Energy Doubler Beam Position Detector,” Proc. 1981 Part. Accel. Conf., *IEEE Trans. Nuc. Sci.* NS**28** (3), 2290-2292 (1981); J. Crisp, “Tev BPM Sources of Error,” talk presented at Fermilab, Beams-doc-812 (August 2003).
- [9] M. Martens, “Position Scan of Tev VPA33 BPM with Upgraded Electronics,” Fermilab Report, Beams-doc-1516 (December 2004).
- [10] R.E. Meller, A.W. Chao, J.M. Peterson, S.G. Peggs, and M. Furman, “Decoherence of Kicked Beams,” SSC Report, SSC-N-360 (May 1987).